# Asymmetric pulses delivered by a cochlear implant allow a reduction in evoked firing rate and in spatial activation in the guinea pig auditory cortex

Victor Adenis, Elie Partouche, P Stahl, D Gnansia, Chloé Huetz, Jean-Marc Edeline


# Asymmetric pulses delivered by a cochlear implant allow a reduction in evoked firing rate and in spatial activation in the guinea pig auditory cortex

V. Adenis , E. Partouche , P. Stahl , D. Gnansia , C. Huetz , J-M Edeline

PII: S0378-5955(24)00080-7
DOI: https://doi.org/10.1016/j.heares.2024.109027
Reference: HEARES 109027

To appear in: *Hearing Research*

Received date: 22 January 2024
Revised date: 30 April 2024
Accepted date: 2 May 2024

Please cite this article as: V. Adenis , E. Partouche , P. Stahl , D. Gnansia , C. Huetz , J-M Edeline , Asymmetric pulses delivered by a cochlear implant allow a reduction in evoked firing rate and in spatial activation in the guinea pig auditory cortex, *Hearing Research* (2024), doi: https://doi.org/10.1016/j.heares.2024.109027

**Highlights**

- Cortical responses evoked by biphasic symmetric and asymmetric pulses were tested
- Asymmetric pulses reduced the cortical responses and spatial cortical activation
- Pulses with a first cathodic phase are more efficient to reduce cortical responses
- The effect was pronounced when the first cathodic phase was of high amplitude
- Asymetric pulses are efficient to focalise cortical responses in cochlear implant

# Asymmetric pulses delivered by a cochlear implant allow a reduction in evoked firing rate and in spatial activation in the guinea pig auditory cortex.

Adenis V.[1,2,3 *], Partouche E.[1,2,3], Stahl P.[4], Gnansia D.[4], Huetz C.[1,2,3], Edeline J-M[1,2,3]

[1] Paris-Saclay Institute of Neurosciences (Neuro-PSI)
[2]CNRS UMR 9197 and [3]Université Paris-Saclay,
91405 Orsay cedex, France
[4] Oticon Medical, Vallauris, France

Corresponding Author: Jean-Marc Edeline; jean-marc.edeline@universite-paris-saclay.fr

UMR 9197, Neuro-PSI (Institut des Neurosciences Paris-Saclay)
Centre CEA Saclay, Bâtiment 151
151 route de la Rotonde
91400 Saclay cedex, France

* present address: Mass. Eye and Ear Institute, Eaton-Peabody Labs,234 Charles St. Boston MA 02114, USA.

## ABSTRACT

Despite that fact that the cochlear implant (CI) is one of the most successful neuro-prosthetic devices which allows hearing restoration, several aspects still need to be improved. Interactions between stimulating electrodes through current spread occurring within the cochlea drastically limit the number of discriminable frequency channels and thus can ultimately result in poor speech perception. One potential solution relies on the use of new pulse shapes, such as asymmetric pulses, which can potentially reduce the current spread within the cochlea. The present study characterized the impact of changing electrical pulse shapes from the standard biphasic symmetric to the asymmetrical shape by quantifying the evoked firing rate and the spatial activation in the guinea pig primary auditory cortex (A1). At a fixed charge, the firing rate and the spatial activation in A1 decreased by 15 to 25 % when asymmetric pulses were used to activate the auditory nerve fibers, suggesting a potential reduction of the spread of excitation inside the cochlea. A strong "polarity-order" effect was found as the reduction was more pronounced when the first phase of the pulse was cathodic with high amplitude. These results suggest that the use of asymmetrical pulse shapes in clinical settings can potentially reduce the channel interactions in CI users.


Keywords: Cochlear implant, Auditory cortex, Electrophysiology, Cortical activation, Pulse shape, Guinea pig.

## 1. Introduction

For several decades, the cochlear implant (CI) has been a neuro-prosthetic device that allowed thousands of patients affected with severe to profound hearing loss to recover hearing sensations and speech understanding. One of the main limitations of this device comes from the electrodes inserted in the scala tympani which are not stimulating independent pools of auditory nerve fibers. The reason is that the current largely spreads when delivering electrical pulses in the perilymph so that adjacent electrodes activate crossed pools of auditory nerve fibers, contributing to limit CI user's speech perception performances (Srinivasan et al. 2014; Arenberg et al. 2018). In addition, safe electric stimulation before chronic setting requires the use of charge-balanced pulses to avoid neural damage (Lilly et al. 1955). All CIs rely on biphasic pulses (meaning each pulse has two phases of opposing polarity) to balance charge and maintain healthy neural tissue over time (Brummer et al. 1977, McHardy et al. 1980 and Loeb et al, 1983). This comes at the price of having twice the charge delivered in a short time window and contributes even more to the current spread. Stimulation modes (i.e., various configurations of active and return electrodes) that aim at focusing the stimulation current such as bipolar (Arnoldner et al. 2008; Bingabr et al. 2014) or tripolar mode (Bierer and Middlebrooks, 2002; Bierer et al. 2010; Goldwyn et al. 2010; see for review Zhu et al. 2012) have been, and are still (Chary et al. 2019), investigated to limit the current spread within the cochlea. Pulse shape is also known to affect the current spread. For example, triphasic pulses were shown to be an efficient way to reduce undesirable facial nerve activation through CI stimulation in patients (Bahmer and Baumann, 2016, Bahmer et al. 2017). Among those new shapes, a promising one, called asymmetrical pulse shapes, are used to study the polarity sensitivity (Carlyon et al. 2015; Macherey et al. 2006, 2008, 2017, Quass et al. 2020, Konerding et al. 2023) and

its relationship with neural survival (Bierer, 2010; Seyyedi et al. 2013; DeVries et al. 2016). Asymmetric pulse shapes are also studied to improve psychoacoustic performance (Chua et al. 2011; Carlyon et al. 2018) or CI fitting (Goehring et al. 2019).

One common approach to quantify this current spread is to determine the spread of excitation (SOE). In theory, the SOE represents the spatial activation of nerve fibers resulting from the stimulation of a given CI electrode. One technique to infer SOE is to estimate the electrodes interaction using forward masking patterns by presenting a masker and a probe stimulus at different electrode locations. One stimulus (the masker) changes location along the array so that it activates different fractions of the auditory nerve fibers at different distances from a fixed stimulation (probe) and prevents them to respond to the probe because of their refractory states when the two stimulations are close enough. Psychophysical studies (Shannon, 1983; Tong and Clark, 1986; Lim et al. 1989; Cohen et al. 1996a; Chatterjee and Shannon, 1998; McKay et al. 1999; Cohen et al. 2001), where the subject's behavioral responses are supposed to reflect the current diffusion within the cochlea, are time consuming and require the patient's active participation. Therefore, over the last two decades, these experiments were performed via objective measures, e.g. via electrically evoked compound action potentials (eCAPs; Frijns et al. 2002; Eisen and Franck, 2005; Hughes and Stille 2008, 2010). Since the eCAP is reflecting the compound activation of the auditory nerve, it was originally assumed that psychophysical tuning reflects the eCAP responses. However, they only accounted for 30% of the psychophysical tuning variance (Cohen et al. 2003). This discrepancy indicates either that eCAPs are not good predictors of psychophysical results (e.g. McKay et al. 2013) or that the methodology used to measure SOE with forward masking is not adequate.

The present study avoids the limits of the forward-masking paradigm by recording CI-evoked cortical responses at different locations of the tonotopic map in the primary auditory cortex of guinea pigs to characterize the impact of asymmetric pulse shapes at the highest level of the auditory system. From this spatial cortical activation, we inferred to what extent the stimulation parameters activated different proportions of the eighth nerve fibers. The goal was to observe if, at high levels of stimulation, asymmetric pulse shapes provide more focused activation of the primary auditory cortex than classical symmetrical pulses. More precisely, cortical activity was simultaneously recorded from 16 different locations (via a matrix of 16 electrodes implanted in A1) and two main quantifications were performed. First, in each cortical location, the evoked firing rate (in spikes/sec) was computed. Second, the spatial activation of the cortical map was constructed from the significant evoked firing rates recorded on the 16 channels. Initially, control experiments were conducted to validate that the cortical response strength and cortical spatial activation are relevant markers of changes in current spread occurring in the cochlea. Indeed, bipolar stimulation is known to be a more focal mode of stimulation associated with a reduction of the spread of excitation within the cochlea (van den Honert and Stypulkowski 1987; Patrick and Clark, 1991) and it was already shown that the cortical spatial activation is reduced by this mode of stimulation (e.g. Bierer & Middlebrooks 2002). After these control experiments, gradual manipulations of the pulse shapes were performed at a fixed charge of 24nC/phase in monopolar mode by introducing an asymmetry, which generated pseudo-monophasic pulses. The asymmetry ratio of square pulses was changed from an amplitude-duration ratio of 1/1 to a 1/10 ratio between the first and second phase. Results showed that changing the ratio of pulses asymmetry significantly reduced the evoked firing rate and spatial cortical activation compared with the classical, symmetrical, square pulses.

## 2. Methods

### 2.1. Subjects

The animals were 22 pigmented Guinea Pigs (*Cavia Porcellus*) from 3 to 19 months old and weighting between 500 to 1150 g, fourteen of which were used for the main study of asymmetric pulse shapes and eight of which were used for control measures. They had a heterogeneous genetic background and came from our own colony housed in a humidity (50-55%) and temperature (22-24°C) controlled facility on a 12 h/12 h light/dark cycle (light on at 7:30 A.M.) with free access to food and water. The animal facility was regularly checked by accredited veterinarians from the Essonne district. The experiments were performed under the national license A-91-557 (project 2014-29, authorization 05202.09) and using the procedures N° 32-2011 and 34-2012 validated by the Ethic committee N°59 (CEEA Paris Centre et Sud). All surgical procedures were performed in accordance with the guidelines established by the European Communities Council Directive (2010/63/EU Council Directive Decree).

The animals' audiograms were determined 2-3 days before cochlear implantation by testing auditory brainstem responses (ABR) under isoflurane anesthesia (2.5%) as previously described (Adenis et al. 2018). The guinea pigs had modest hearing loss (20 dB in the worse cases) corresponding to their age (Gourévitch et al. 2009, Gourévitch & Edeline 2011).

### 2.2. Cochlear implantation and cortical surgery

The surgery was performed under general anesthesia induced by Urethane (1.2 g/kg, i.p.) and supplemented by lower doses (0.5-0.7g/kg) when reflex movements were observed after pinching the hind paw. Each animal was initially placed in a stereotaxic

frame for the craniotomy. A heating blanket allowed maintaining the animal's body temperature around 37°C. After injection of a local anesthetic (Xylocaine 2%, s.c.), the skin was opened, and the temporal muscles were pushed on the side. The skull was cleaned, then dried, and four stainless steel screws were threaded into burr holes in the calvarium to anchor a miniature socket (10 x 3 x 3mm) embedded in dental acrylic cement. A craniotomy was performed on the left temporal bone, 5mm behind the Bregma on the rostro-caudal axis to expose the primary auditory cortex; the opening was 8-10 mm wide. The skin behind the right pinna was opened and the tympanic bulla was exposed. The bulla was opened under binocular control with a 2 mm cutting burr (mounted on a surgical drill) and the cochlea orientation was determined based on anatomical landmarks (round window). A cochleostomy was then performed around 1 - 1.5 mm below the round window with a 0.4 mm diameter trephine.

The animal was implanted with a head connector including a shortened version of the EVO electrode array used by Oticon Medical (Smørum, Denmark, see Nguyen et al. 2012) and a 70mm tubing ending with a large surface ball of Platinum-Iridium used as the extracochlear ground. The array (300µm diameter) was composed of 6 ring-shaped Platinum-Iridium electrodes of the same diameter for a 0.0046 $mm^2$ surface. Center-to-center inter-electrode distance was 600 µm. The head connector was secured on the calvarium with acrylic cement and the ground electrode inserted below the skin, between the animal's shoulders. The array supporting the six intracochlear electrodes was then inserted into the scala tympani. A visual confirmation of the number of inserted electrodes in the cochlea was made by direct observation through the binocular microscope. In all cases, five electrodes were inside the cochlea with the sixth being on the edge of the cochleostomy. Electrode impedances were measured before starting the stimulations and always ranged from 2kΩ to 4kΩ. Recordings of the eCAP were

performed immediately after surgery for each of the six electrodes to check the post-insertion electrode interface integrity. Note that, as the animals were part of another experiment which required quantifying their residual hearing (Partouche et al. 2022), they were not deafened prior to the cochlear implantation and during data acquisition.

### 2.3. Responses of auditory cortex neurons

Neural activity was recorded in the left primary auditory cortex (A1). Methodologies and procedures for data acquisition were identical to those described in our previous studies (Gaucher et al. 2013; Occelli et al. 2016; Aushana et al. 2018). Briefly, a 16-channels electrode matrix (ø: 33 µm, <1 MΩ), composed of two rows of 8 electrodes separated by 1000 µm (350 µm between electrodes of the same row), was inserted in A1 perpendicularly to the cortical surface to record multi-unit activity at a depth of 500-600µm (corresponding to layer III/IV according to Wallace and Palmer 2008). A small silver wire (ø: 200µm), used as ground, was inserted between the temporal bone and the dura matter on the contralateral side. The location of A1 was estimated based on the pattern of vasculature observed in previous studies (Edeline et al. 1993, 2001; Manunta and Edeline 1999; Souffi al. 2020, 2021, 2023). The raw signal was processed as in Adenis et al. (2018). The signal was amplified 10,000 times (TDT Medusa) and processed by an RX5 multichannel data acquisition system (TDT). The signal collected from each electrode was filtered (610-10000 Hz) to extract multi-unit activity (MUA). A trigger level was set for each cortical electrode to select the largest action potentials from the signal. Careful on-line and off-line examination of the waveforms indicated that the MUA collected in our experiments was most likely made of action potentials generated by 2 to 6 neurons at the vicinity of the electrode. For each experiment, the position of the electrode array was set in such a way that the two rows of eight

electrodes sampled neurons responding from low to high frequency when progressing in the rostro-caudal direction. An example of tonotopic gradient observed in one of our experiments is presented on Figure 2 (see also other examples of tonotopic gradients recorded with such arrays in our previous studies: in Gaucher et al. 2012 and in Occelli et al. 2016). To ensure the good placement of the electrode array, tonal frequency response areas (FRA) were measured by presenting 50ms pure tones at 2Hz, from 0.25 to 36kHz and from 5 to 75dB SPL.

### 2.4. Stimulation protocols

The stimulation protocols were controlled via a research platform designed by Oticon Medical (Smørum, Denmark, designed at Vallauris, France) and connected to the implant by the head connector secured on the animal's head. Single pulses were delivered at 4Hz in a monopolar mode via the most apical electrode (named E0 in the following).

In control experiments, comparisons were made between the responses obtained with monopolar (MP) and bipolar (BP+1, stimulation between E0 and its closest neighbor electrode, named E1) modes of stimulation. Anodic- and cathodic-first rectangular biphasic pulses were presented at 20 levels of charge ranging from 3 to 31.5 nC per phase in either an MP or a BP+1 configuration. The charge was increased through the phase amplitude (current), which ranged from 100 μA to 1050 μA (increments of 50 μA/phase) with fixed phase duration of 30 μsec/phase and an interphase gap of 15 μsec. This control experiment aimed at evaluating whether our cortical recordings allowed visualizing the smaller current spread that is generated in the cochlea by the BP mode of stimulation compared to the MP mode.

In a second set of experiments, rectangular charge-balanced biphasic pulses were used at a fixed charge of 24nC per phase in a MP configuration. It was selected as it corresponds to the mean saturation level of cortical firing rate in control experiments. The ratio of asymmetry between the first and the second phase of the pulse ranged from 1/1 (symmetrical pulse) to 1/10 (asymmetrical pulse; see Fig. 1.A) and was increased step-by-step (with 8 intermediate values). A 1/10 ratio corresponds to one phase being 10 times smaller in phase amplitude and 10 times longer in phase duration than the other phase of the same pulse so that the total charge injected per phase remained balanced. The configuration of the pulse was also modified so that the asymmetry was applied at different phases to create Anodic Short First (ASF), Cathodic Short First (CSF), Anodic Long First (ALF) and Cathodic Long First (CLF) pulses (Fig. 1.B). This resulted in 40 pulse shapes in total (10 ratios, 4 configurations).

The order of presentation of each pulse shape (ASF, ALF, CSF, CLF) was randomized from one position of cortical electrode array to the next and there were periods of 30-60sec between each type of pulse shape to minimize habituation or desensitization of the cortical responses.

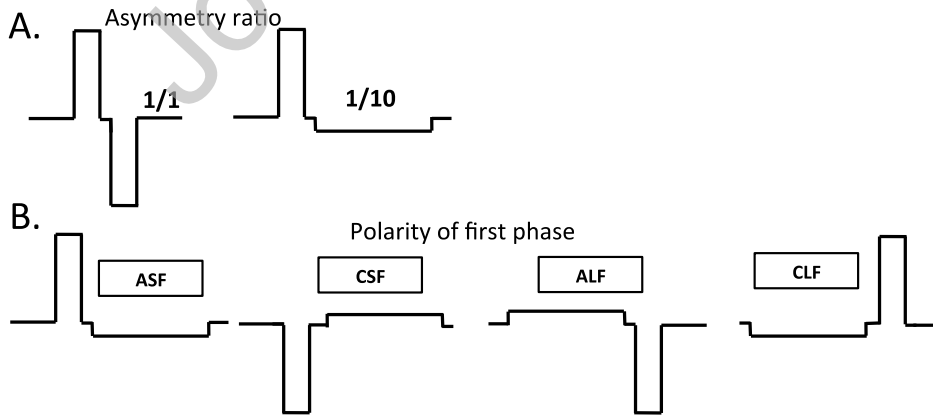


**Figure 1.** Schematic diagrams representing the different pulses configurations used in our study.

A. Schematic comparison between the shape of the square symmetric pulse with a 1/1 ratio and the most asymmetric pulse shape (1/10) where the amplitude of the second phase was 1/10 of the first (and its duration 10 times longer for keeping the charge balanced).
B. Representation of the four pulse configurations used in the present study depending on whether the first phase was short (ASF and CSF) or long (ALF and CLF) for both tested polarities. ASF: Anodic Short First. CSF: Cathodic Short First. ALF: Anodic Long First. CLF: Cathodic Long First.

### 2.5. Quantification of cortical responses: Evoked firing rate and spatial activation

During offline analyses, the cortical evoked firing rate triggered by each pulse shape and by each ratio of asymmetry was quantified between 5 and 45ms after pulse onset. The evoked firing rate (FR, number of action potentials per second) obtained for each cortical electrode was averaged across the 64 repetitions of each condition (pulse shape and ratio). A cortical recording was considered to generate significant responses when the evoked activity was 6 SD above its spontaneous firing rate. The FR values obtained from each cortical recording were averaged for each condition across electrodes and animals to obtain group data. To compare the changes in evoked FR across all the asymmetry ratios, we computed the percentage of change in FR relative to the firing rate obtained for the 1/1 ratio.

Changes in firing rate and in spatial activation (SA) were further analyzed. In the control experiments, both the FR and the SA were quantified at the maximum charge, i.e. at 31.5nC, and will be referred to as $FR_{31.5nC}$ and $SA_{31.5nC}$ in the results. For the second set of experiments, the FR and SA quantifications were based upon the responses obtained with the most asymmetric (1/10) vs. the symmetric (1/1) pulse. The changes in firing rate were computed based on the FR obtained for each cortical electrode exhibiting significant responses. The spatial activation (SA) was computed as the distance (in mm) where significant evoked responses were detected from one array of 8 cortical

electrodes to obtain the extent of the cortical activation across the rostro-caudal tonotopic gradient.

To obtain a more direct evaluation of the potential increase in frequency selectivity that can be generated using asymmetric pulses, we transformed the millimeters of spatial activation into octave ranges. Based on several papers describing in details the tonotopic representation in the primary auditory cortex of guinea pigs (Roberston & Irvine 1989; Redies et al 1989a,b; Wallace et al 2000; 2002) as well as our previous studies (Manunta & Edeline 2001; Gaucher et al 2013; Occelli et al 2016; Souffi et al 2021, 2022, 2023), the spatial activation was transformed in an octave basis (using as a metric that the 2.5mm of rostro-caudal extent of A1 covers the 6 octaves of frequencies represented in the guinea pig auditory cortex).

### 2.6. Statistical analyses

The data did not follow a normal distribution (Shapiro-Wilk tests) and thus required non-parametric testing. The experimental design called for the use of Repeated Measure ANOVAs (RM-ANOVAs). Data was first aligned and ranked using the ARTool software (Wobbrock et al., 2011) then fed to the teg_RMA algorithm (Gladwin, 2020) to carry non-parametric RM-ANOVAs. When appropriate, Wilcoxon signed rank (WSR) tests were used with $p < 0.05$ (alpha= 5%) as significance threshold. In case of multiple tests and to ensure the validity of the effects, the results went through Benjamini-Hochberg corrections to take the false detection rate into account. Chi-square tests were also conducted on the different proportions of spatial activation and a level of $p < 0.05$ was used to assess the significance value. All tests were performed with MatLab 2021b or GraphPad (Prism).

## 3. Results

The acoustic threshold and frequency tuning of all recording's sites were characterized before assessing electrical stimulation. The tonotopic gradient established before insertion of the cochlear implant and the short response latencies to pure tones (<20ms) clearly confirmed the placement of recording electrodes in A1 (figure 2). Before describing the effects of asymmetric pulse shapes on the responses of auditory cortex neurons, we will first show that the cortical responses can be relevant markers of the extent of the current spread in the cochlea.

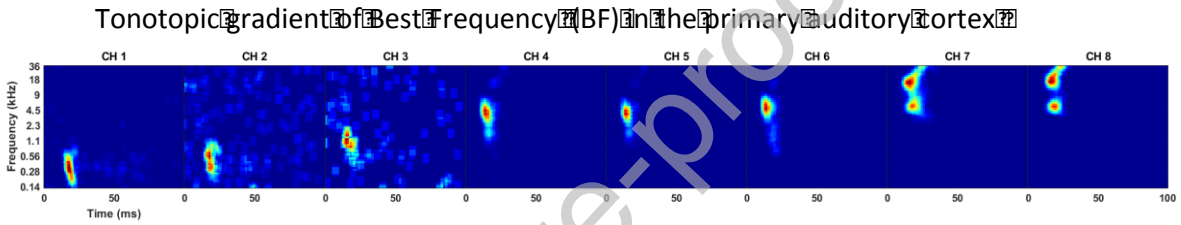


Figure 2. Example of tonotopic organization in the primary auditory cortex based on spectrotemporal receptive fields. Simultaneous recordings were obtained in the guinea pig primary auditory cortex at eight different locations. The MultiUnit Activity (MUA) was recorded with an array of 8 electrodes placed along the rostro-caudal axis. Spectrotemporal receptive fields were obtained by presenting pure tones from 140Hz to 36kHz. White contour circles indicate evoked firing rates above spontaneous activity plus 6 SD. Note that the receptive fields are from low to high frequencies when progressing from the rostral to the caudal part of A1.

### 3.1. Control Experiment: Cortical response strength and cortical spatial activation as cortical markers of the current spread in the cochlea.

For this control experiment, data come from 8 guinea pigs from which cortical multiunit recordings were collected for a total of 14 positions of the 16-channels electrode matrix in A1. Only cortical sites presenting evoked responses to both monopolar and bipolar stimulations were compared. Figure 3 shows the mean evoked response obtained with Monopolar (MP) and Bipolar (BP+1) stimulations, when using Anodic-first or Cathodic-first pulses. The $FR_{31.5nC}$ was significantly lower for BP+1 than for MP (Fig. 3.A), both for

anodic and cathodic first pulses (WSR test, MP vs. BP +1, p-value = 0.0003 for anodic-first pulses and p-value =0.0029 for cathodic-first pulses). The $SA_{31.5nC}$ (Fig. 3.B) observed using the BP + 1 mode was significantly smaller than the SA evoked by the MP mode, independently of the polarity scheme (WSR test, MP vs. BP +1, p-value = 0.02 for anodic-first pulses and p-value = 0.04 for cathodic-first pulses).

These results show that our measures of cortical activity quantified by the firing rate and by the spatial activation, can be used for estimating differences in current spread occurring within the cochlea: a mode of stimulation known to be more focal, namely the bipolar mode (BP+1 mode) compared to the monopolar mode (MP), reduced both the firing rate and the spatial activation in the primary auditory cortex.

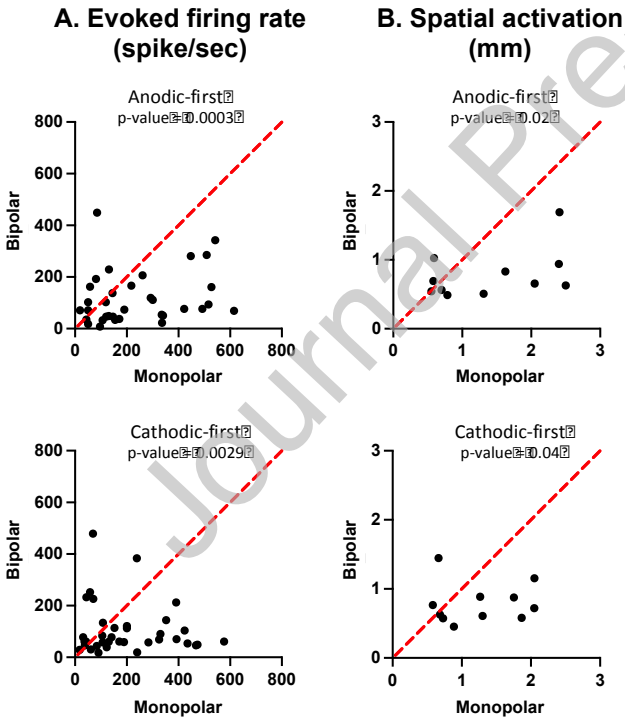


*Figure 3. Comparison between the effects generated by the Monopolar (MP) and the Bipolar (BP) stimulation mode at the level of A1.*

*A. Scattergrams comparing the evoked firing rates (FR in spike/sec) obtained at 31.5nC using monopolar (MP, abscissa) vs. bipolar (BP, ordinates) stimulation mode for anodic-first (Top left) and cathodic-first pulse (Bottom left). On average, BP evoked lower FR than MP for both polarity schemes.*

*B. Scattergrams comparing the spatial activations (in mm) obtained at 31.5nC using either MP (abscissa) or BP (ordinates) stimulation mode for anodic-first (Top right) and cathodic-first pulse (Bottom right). On average, BP evoked smaller SA than MP with both polarity schemes.*

### 3.2. Effect of pulse asymmetry.

#### 3.2.1. Cortical evoked firing rate (FR) with the four asymmetric pulse shapes.

Data used for the comparison between symmetrical and asymmetrical pulses comes from 14 guinea pigs, from which 1437 cortical multiunit recordings were collected during 119 positions of the 16-channels cortical matrix. For these 1437 recording sites, evoked responses were obtained with a constant charge of 24nC per phase with the four configurations of rectangular asymmetric pulses (see in Figure 1B) while changing the asymmetry ratios. The raster plots presented on figure 4A illustrate two examples (from two different animals) of cortical evoked responses to the 10 ratios of asymmetry from the symmetrical shape (1$^{st}$ level, bottom) to the 1/10 ratio (top). In both examples, it can clearly be observed that the number of action potentials elicited at each trial (i.e. at each electrical pulse delivered in the cochlea) is larger with the 1/1 ratio (bottom) than with the 1/10 ratio (top). The quantifications of these evoked responses are presented in figure 4B. Note that in both cases, the evoked firing rate progressively decreased as if the electrical pulses progressively activated fewer auditory nerve fibers, but still remained efficient to elicit cortical responses. For the first recording displayed in figure 4 (left on Fig. 4A and top of Fig. 4B), the evoked firing rate decreased until the last two ratios of asymmetry, whereas on the second example (Fig 4A right and Fig 4B bottom), the evoked firing rate decreased until the 5$^{th}$ ratio of asymmetry, then stayed at the same level, or even showed a slight recovery.

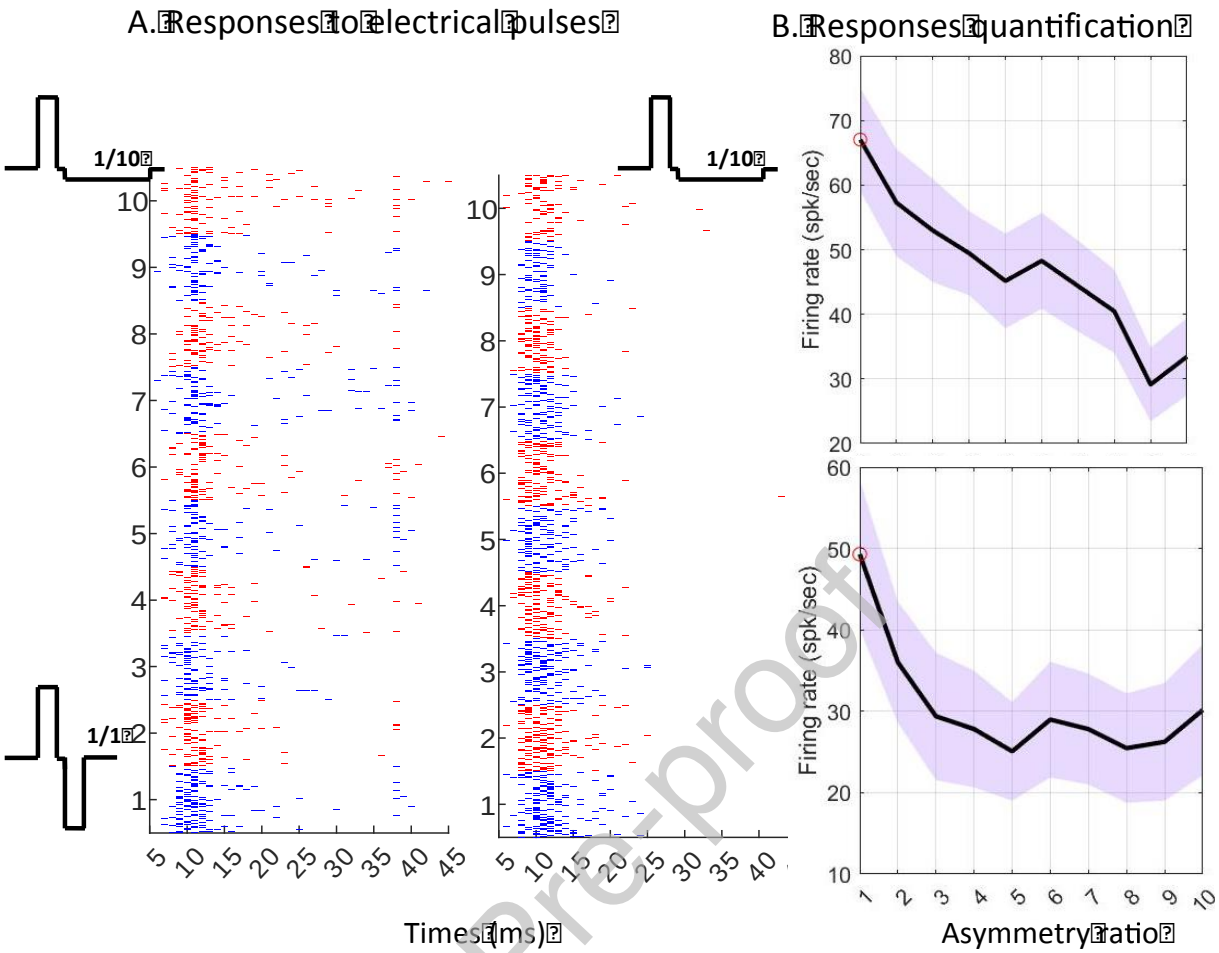


*Figure 4. Raster plots (A) and quantification of evoked responses (B) for two individual recordings.*

- *A. Raster plots of two individual recording sites showing evoked responses triggered by each ratio of asymmetry (from 1/1, bottom to 1/10, top) for the ASF shape (A1, A2). Alternating colors represent the different levels of asymmetry with the 64 repetitions of for each level.*
- *B. Corresponding mean evoked firing rates (spikes/sec) observed for these two recordings (black curves) and their associated standard deviation (purple field) for each ration tested (top and bottom curves correspond respectively to left and right raster plots). Red circles indicate the maximum observed FR. In both case, the mean FR decreased as the ratio of asymmetry increased, with ratio 1/1 (symmetric pulse) evoking the maximum firing rate.*

To compare the consequences of changing the asymmetry ratio on the population of recordings, the mean firing rate changes were expressed in percentages using the 1/1 ratio as reference point. Figure 5 shows that compared with the symmetric shape (1/1 ratio), all the other ratios evoked systematically lower firing rates, whatever the pulse shapes.

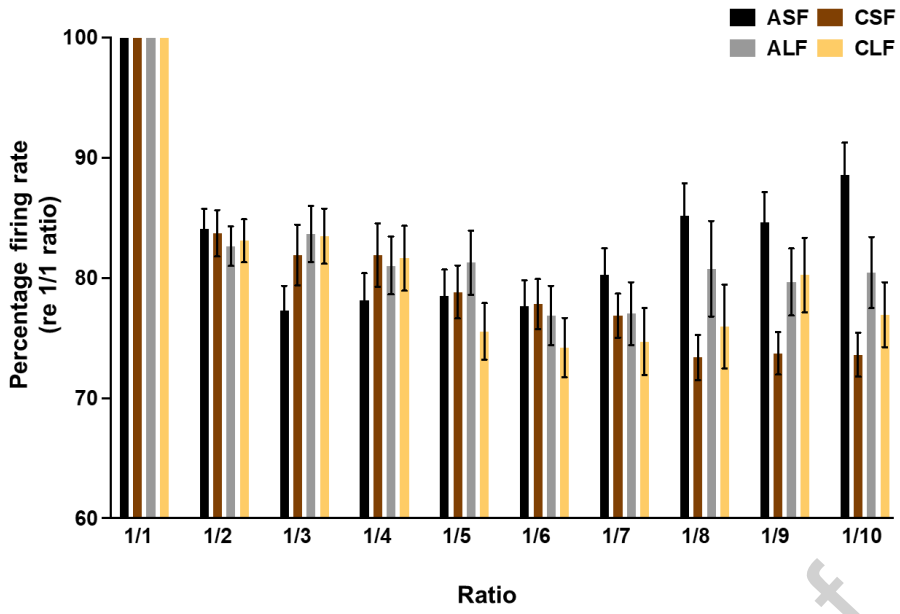


*Figure 5. Evolution of cortical evoked firing rate as a function of the pulse asymmetry.*

*For each asymmetric pulse shape tested (ASF: black, CSF: brown, ALF: grey, CLF: yellow), evolutions of the mean evoked firing rate (+SEM) are represented as percentages using the symmetric pulse shape (ratio 1/1) as a reference point. In general, all asymmetric pulse shapes evoked lower firing rates as the ratio of asymmetry increased. The magnitude of the reduction however differed within each pulse shape (maxima: 23% decrease for ASF, 24% decrease for ALF, 26% decrease for CLF at ratio 1/6 and 27% decrease for CSF at ratio 1/7).*

A two-factors RM-ANOVA revealed that there was a significant firing rate decrease with the asymmetry ratio ($F(9,117)= 23.3$, $p= 3.3*10^{-10}$), no significant effect but a tendency for the pulse shape factor ($F(3,39)= 2.5$, $p= 0.088$), and a significant interaction ($F(27,351)=3.0$, $p= 0.0023$) between these two factors. The factor 'pulse shape' was divided in two factors: the polarity of the first phase ('Polarity') and the duration of the first phase ('Duration'). A two-factors RM-ANOVA between factors Polarity and Ratio yielded a similar result: The asymmetry ratio had a significant effect ($F(9,117)= 15.6$. $p= 4.7*10^{-8}$), Polarity only showed a tendency ($F(1,13)= 3.3$, $p= 0.091$) but an interaction existed between these two factors ($F(9,117)= 3.8$, $p=0.029$). On the other hand, a two-factors RM-ANOVA between factors Duration and Ratio showed that both factors had a significant effect on the firing rate changes ($F(1,13)= 5.5$, $p=0.035$ and $F(9,117)= 11$, $p= 5.2.10^{-6}$, respectively) coupled with an interaction ($F(9,117)= 4.9$, $p= 0.014$).

These statistical analyses pointed out that the evolution of the FR changes across levels of asymmetry differed for the four pulse shapes. On average, at equivalent charge per phase, the asymmetrical shapes reduced the evoked response by 11 to 27% compared to the classical symmetrical shape (WSR tests, 1/1 vs. 1/10, all p-values < 0.0001). For the CSF pulse shape, the evolution of FR with asymmetry almost followed a monotonic-like decreasing slope up to a plateau around the 1/7 to 1/8 ratios. However, the ASF and ALF pulse shapes produced a marked U-shape curve with the FR reaching a minimum around 1/6 (with a maximal decrease of 23% and 24% of the cortical evoked response respectively). It was also the case, but to a lesser extent, for the CLF pulse shape (with a maximal decrease of 26% of the evoked response for the 1/6 ratio).

### 3.3. Reduced evoked firing rate (FR) and spatial activation (SA) with the asymmetrical pulses.

The decrease in firing rate (FR) observed between the 1/1 and 1/10 ratio was often accompanied by a reduction of the spatial activation within the primary auditory cortex. Two individual recordings showing strong decreases in FR from the 1/1 to the 1/10 ratio are presented on Figure 6.A. The associated spatial activations of the cortical map are displayed in Figure 6.B: the spatial activation was clearly reduced in both cases (see the values in white in top and bottom of Fig. 6.B).

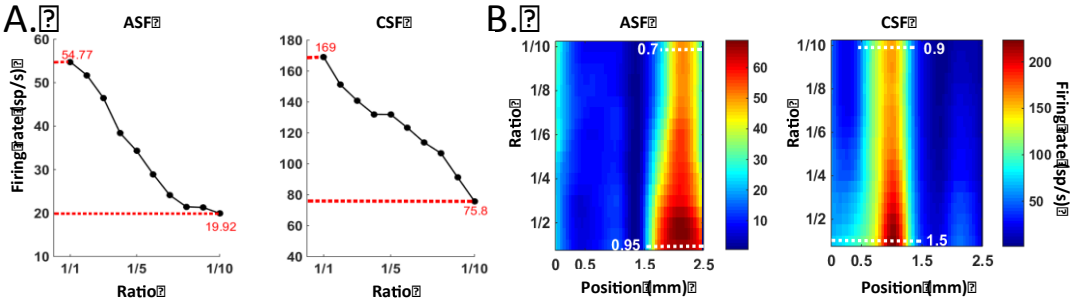

*Figure 6. Individual examples of firing rate decrease (A.) and spatial focalization of cortical activation (B.) for the different ratios of asymmetry.*
*A. The mean evoked firing rate (FR) of two cortical sites is plotted as a function of the asymmetry ratio from the 1/1 symmetrical ratio to the 1/10. For these two examples, the FR decreased whatever the pulse configuration was (left: ASF, right: CSF).*
*B. Cortical spatial activation obtained for the different ratios of asymmetry from the 1/1 to the 1/10. The two examples displayed in A correspond to the cortical activation displayed in B (Left: ASF, right: CSF). There was a clear reduction in cortical spatial activation when the asymmetry ratio increased (from 0.95 to 0.75 mm with the ASF and from 1.5 to 0.9 with the CSF).*

The group data are presented in Figure 7A with the values of evoked firing rate for the 1/1 ratio (abscissa) against the values for the 1/10 values (ordinates), separately for the four asymmetrical pulse shapes presented in figure 1 (i.e. ASF, CSF, ALF, CLF). These scattergrams confirm that for a vast majority of recordings, the firing rate was lower for the asymmetric pulse shapes than for the symmetric ones (WSR, all p-values < 0.0001).

Group data also confirmed the reduction in spatial cortical activation from the 1/1 to 1/10 for the asymmetric pulse shapes (Figure 7.B). The scattergrams presented in this figure display the values of covered frequency ranges for the 1/1 ratio (abscissa) against the values for the 1/10 ratio (ordinates), separately for the four asymmetric pulses presented in figure 1 (i.e. ASF, CSF, ALF, CLF). These scattergrams indicate that, except for the ASF pulses, there was a large majority of cases for which the range of frequencies activated on the tonotopic map was smaller for the asymmetric pulses than for the symmetric ones (WSR, p-values < 0.0001 for CSF and CLF, p-value = 0.0021 for ALF), excepted for ASF (WSR, p-value = 0.93).

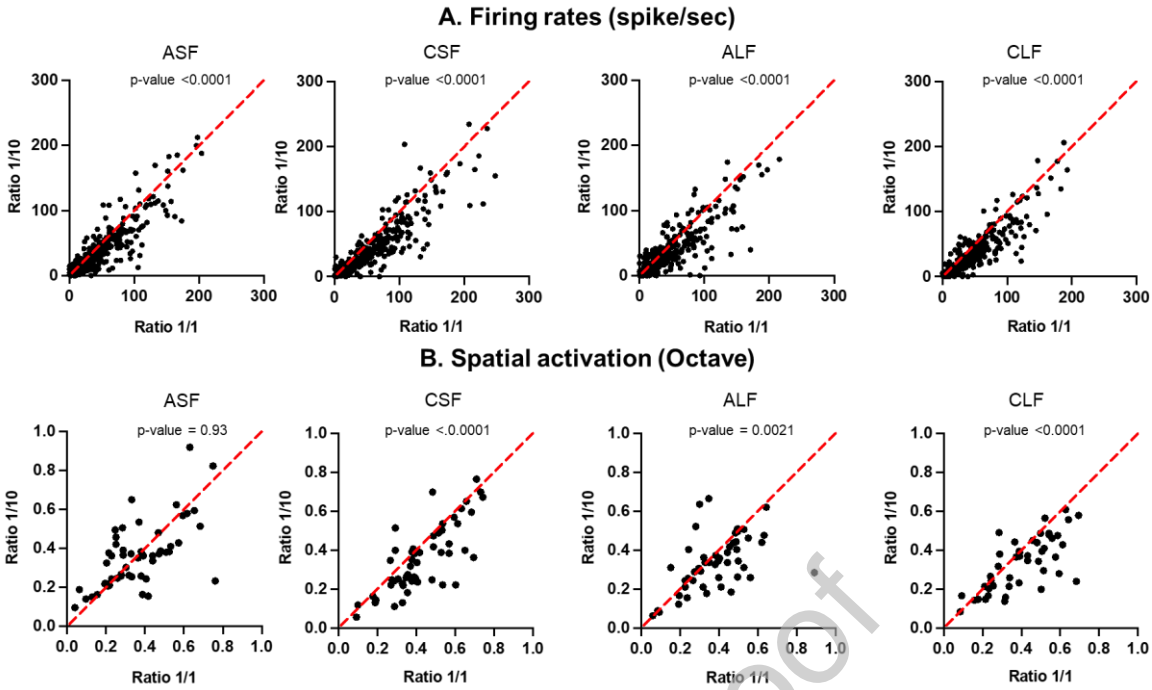


Figure 7. Group data showing decreased firing rate (A) and frequency range (B) with the use of asymmetric pulse shapes. In both cases, except for ASF, most recordings showed lower values for asymmetric pulse shapes.

A) Scattergrams comparing the mean firing rates observed between ratios 1/1 and 1/10, for each asymmetric pulse shape tested (from left to right: ASF, CSF, ALF, CLF). The red line is the equality line.

B) Scattergrams comparing the frequency ranges (in octaves) covered by spatial activation between ratios 1/1 and 1/10 for each asymmetric pulse shape tested (same order as A). Red line represents the equality line. Note that reductions of frequency range up to 0.6 octaves have been observed.

In summary, increasing the ratio of asymmetry usually, but not systematically, reduced both the evoked firing rate (FR) and the spatial activation in A1.

### 3.4. Local changes in spatial activation with asymmetric pulse shapes.

Careful examination of the individual cases of cortical activation indicated that the evolution of the FR and SA when using asymmetric pulses was not uniform across animals. In fact, three different profiles of activation were observed (Fig. 8):

- Focalization (FO, Fig. 8.A): it corresponds to monotonic decreases in FR and in spatial activation from the 1/1 to the 1/10 ratio of asymmetry. Except for the ASF pulse shape, the FO category was the dominant category for the three other pulse shapes (see also Figure 4A-B).
- Expansion (EX, Fig. 8.B): it corresponds to monotonic increases in FR and in spatial activation from the 1/1 to 1/10 ratio of asymmetry.
- Local Focalization (L-FO, Fig. 8.C): it corresponds to non-monotonic decreases in firing rate, with a minimum value in FR and in spatial activation for an intermediary ratio of asymmetry. The example provided in Figure 8.C showed minimum values at ratio 1/6 (see also Figure 4A2-B2).

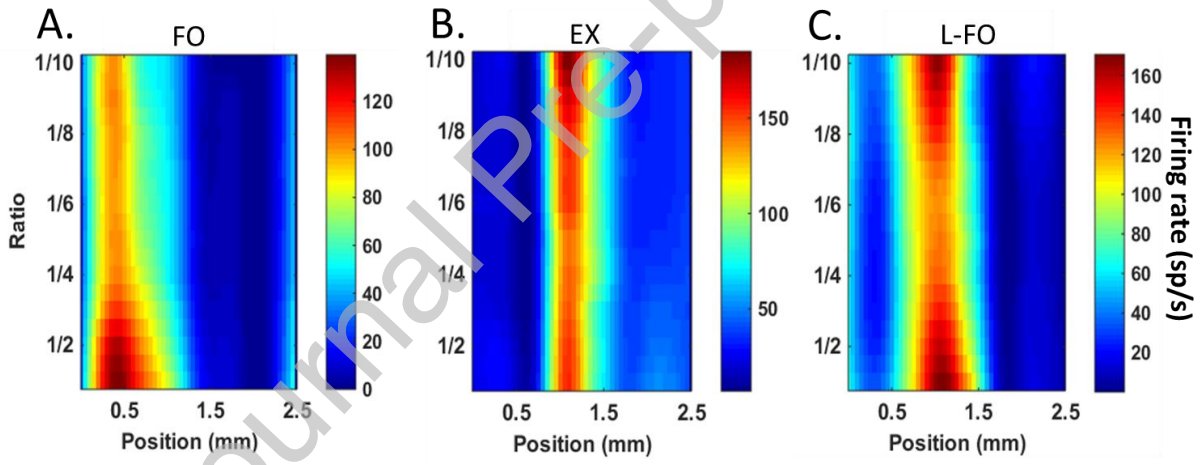


*Figure 8. Individual examples illustrating the three profiles of spatial activation (A-C) obtained when changing the ratio of asymmetry.*
*A. The focalization category (FO) represented a reduction of the firing rate and spatial activation at the 1/10 ratio compared with the 1/1 ratio. CSF shape used.*
*B. The expansion category (EX) represented an increase of the firing rate and an enlargement of the spatial activation at the 1/10 ratio compared with the 1/1 ratio. ASF shape used.*
*C. The local focalization category (called L-FO) represented a maximal reduction of the firing rate and spatial activation at a particular ratio of asymmetry (instead of the ratio 1/10) compared with the 1/1 ratio. ALF shape used.*

As shown in Table 1, a small proportion of profiles fit neither with the FO, nor with the L-FO, nor with the EX criteria and have been named “Others”. This category includes (i) cases of stability for the firing rate and spatial activation when changing the asymmetry

and (ii) increases or decreases in firing rate occurring for a particular ratio of asymmetry without change in spatial activation. On a given animal, opposite profiles were never observed on the two parallel arrays of 8 electrodes. The profiles were either of the same type on the two arrays or a FO type (or EX type) for one array and an "Other" type for the other array. A statistical analysis based on the different proportions of theses profiles confirmed that both cathodic-first pulse shapes significantly reduced the spatial activation in A1 (especially the cathodic long first, CLF, which produced 60% of FO profiles). The proportion of profiles differed significantly between ASF and CLF (Chi-Square = 16.75, $p < 0.001$). It also differed between the ALF and the CLF shape (Chi-Square = 10.06, $p < 0.05$). This indicates that there is a tendency for a higher proportion of EX profiles with the anodic first pulse shapes.

| | **ASF** | **CSF** | **ALF** | **CLF** | **Total** |
|---|---|---|---|---|---|
| **EX** | 21 (38.88%) | 11 (21.15%) | 13 (26.53%) | 3 (8.11%) | 48 (23.72%) |
| **FO** | 17 (31.5%) | 25 (48.1%) | 20 (40.81%) | 22 (59.45%) | 84 (46.06%) |
| **Local FO** | 14 (25.92%) | 11 (21.15%) | 14 (28.57%) | 6 (16.22%) | 45 (23.25%) |
| *Total FO* | *31 (57.42%)* | *36 (69.25%)* | *34 (69.38%)* | *28 (75.67%)* | *129 (69.31%)* |
| **Others** | 2 (3.7%) | 5 (9.6%) | 2 (4.09%) | 6 (16.22%) | 15 (6.97%) |
| **Total** | 54 (100%) | 52 (100%) | 49 (100%) | 37 (100%) | 192 (100%) |

Table 1. Proportions of observed profiles for each tested asymmetric pulse shape
Proportions of observed profiles of spatial activation for each pulse shape are displayed in this table. The associated percentages are also provided in parenthesis for each pulse shape and for each profile across pulse shapes (Last Column). The Total FO total represents the summation of FO and L-FO profiles.

The FO and the L-FO profiles can potentially be grouped together. Grouping these two categories points out that the dominant effect of asymmetric pulse shapes is indeed a reduction of the cortical firing rate and spatial activation. The total FO profiles (including the local FO) represented a large majority of the observed profiles when the pulse shape became asymmetrical (with 57%, 69%, 69%, 75% of occurrence for ASF, CSF and ALF, CLF, respectively). Note that the ASF configuration generated the lowest percentage of FO occurrences (only 31.5%), which is in good accordance with the

evolution of the mean firing rate presented in figure 5. Taken together, these results suggest that the largest ratio of asymmetry used here (1/10) is not always the best to reduce cortical activation.

## Discussion

In the present study, we show that, at a constant charge, cortical responses evoked by electrical cochlear stimulation are influenced by the shape of the electrical pulses. Specifically, going from the standard symmetric biphasic pulse shape to asymmetric biphasic pulse shapes reduced the evoked responses and the spatial activation in the primary auditory cortex without changing the injected charge. To our knowledge, this is the first time that asymmetric pulses are shown to impact cortical responses (but IC recordings and eCAPs have been tested with asymmetric pulses, see Quass et al 2020; Konerding et al 2023). Although this can be viewed as an indication of a lower efficiency of asymmetric pulses for coding sound loudness, we propose that the decrease in spatial activation observed at the cortical level can be interpreted as a potential consequence of a decrease in the spread of activation within the cochlea.

### 3.2. Sensitivity to pulse shape, polarity and order.

Several human and modeling studies showed that the polarity scheme plays an important role in the efficiency of cochlear implant stimulation. In humans, it is usually admitted that cathodic currents are more effective in depolarizing the peripheral terminals of spiral ganglion neurons (SGN), whereas anodic currents are effective in depolarizing SGN somas (Rattay et al. 2001a,b; Resnick et al. 2018). Although these studies were mostly based on models, both peripheral terminals and somas were suspected to be suitable initiation sites of action potentials based on evoked response latencies (Javel & Shepherd, 2000), but as the peripheral terminals are closer from the stimulating electrodes than the soma, their activation (when they are still present) should lead to lower thresholds with cathodic currents. Lower threshold potentially generates smaller spread of excitation. This difference was studied through the use of

asymmetrical pulse shapes at threshold current levels (Macherey et al. 2017, Carlyon at al. 2018) and it is now proposed as a potential tool to assess neural degeneration in CI users under the terms of "polarity effect" (Mesnildrey et al. 2020, Jahn & Arenberg 2019, 2020). However, at supra-threshold levels, CI users are mostly sensitive to anodic stimulation due to the action potential initiation occurring at the soma (Macherey et al. 2008; van Wieringen et al. 2008; Undurraga et al. 2010; Hughes et al. 2017, 2018). Thus, at high intensity of stimulation, the "polarity effect" might not provide much information about health of the peripheral terminals. Nonetheless, one must keep in mind that direct comparison between human data (where substantial degeneration of peripheral processes can exist) and our data (where there is no such degeneration) is difficult.

Here, the reduction of the evoked firing rate and spatial activation confirms that asymmetrical pulses modulate cortical spatial activation at high intensities of stimulation, which is an important result when aiming at reducing the current spread, or at least the SOE. In humans, reliable quantifications of the SOE are difficult because the peripheral measures (e.g., eCAP) can be masked by the long artifact duration. Also, it is not easy to implement asymmetrical pulses in clinical settings (Spitzer et al. 2019). Cortical recordings in animals present several advantages over traditional eCAP recordings and psychoacoustic methods. First, cortical responses are obtained without complex subtractions required to remove the stimulation artifact when quantifying the eCAP. Second, the different percentages of cortical spatial activation reported here as a function of the pulse shape (ASF, ALF, CSF and CLF) confirm that the polarity scheme has physiological consequences in the central auditory system. Last, it has been documented that the spatial activation of the primary auditory cortex (A1) is related to perceptive abilities (Recanzone et al. 1993; Reed et al 2011; Rutkowski & Weinberger 2005

Bieszczad & Weinberger 2010; review in Edeline 1999, 2003) whereas this has been questioned for the eCAP amplitude and threshold (see McKay et al. 2013).

Several points must be considered in light of our results. In humans, Spitzer & Hughes (2017) found that for equal current levels in CI users, anodic-first pulses evoked broader SOE than cathodic-first pulses for symmetrical biphasic pulses. In animal models, cathodic currents preferentially depolarize SGN somas whereas anodic currents preferentially depolarize the peripheral processes (Miller et al. 1998, 1999 and 2004). Two of our observations are consistent with these findings. Firstly, cathodic-first symmetrical pulses (1/1 ratio) evoked a broader spatial activation in A1 than anodic-first pulses (WSR, p-value = 0.0349, data not shown). Secondly, cathodic-first pulses also tended to generate larger reductions in spatial cortical activation when the pulse shape was changed from the symmetrical (1/1 ratio) to asymmetrical shape (1/10 ratio, Figure 7B) suggesting that for high stimulation levels, the asymmetrical pulse shape reduced primarily the recruitment of SGN somas and effectively reduced the spread of activation (in accordance with Rattay et al. 2013, see also Heshmat et al. 2021).

With asymmetrical pulses, and at equal charge, the effectiveness of the long phase with low amplitude to trigger action potentials is lower than the effectiveness of the short, high amplitude, phase (Macherey et al. 2006). For high values of asymmetry, neural responses mostly come from the high amplitude/short duration phase of the pulse (Miller et al. 2001), independently of the polarity of the phase (Undurraga et al. 2013). Some of our results do not match with this hypothesis: when using the ASF and the CLF shapes, in both cases the cathodic phase was the long-duration and low-amplitude phase but their position differed. Thus, at the 1/10 ratio, the evoked responses should be equivalent for ASF and CLF. This is not the case, and the same observation holds true

between the CSF and ALF shape. The dynamics of both the firing rate and spatial activation differed between the different shapes, indicating that both the position and also the order of the phases inside the pulse are important.

A recent set of experiments by Guérit and colleagues (2018, 2020) showed an "order effect" on loudness perception of paired pulses with the use of different asymmetrical pulse shapes at short inter-pulse interval (below 345µs). They replicated the findings of Spitzer & Hughes (2017) and Todd & Landsberger (2018) but also showed that the order effect disappeared at short inter-pulse intervals if the long-low amplitude phases were removed or if using symmetric pulses. Here, our observations of different cortical activation profiles when changing the asymmetry ratio and polarity scheme clearly suggest an effect within the pulse itself, akin to the order effect mentioned above. For example, in the ASF and CLF conditions, the cathodic phase is reduced but does not have the same location within the pulse (first in CLF but second in ASF) and led, respectively, to a higher percentage of expansion (EX) of cortical activation with the ASF shape and a higher percentage of focalization (FO) with the CLF shape. To summarize, when using asymmetrical pulses, the order of the phases and their respective amplitude-duration ratio, have different consequences on the cortical spatial activation, in coherence with past experiments.

### 3.3. Potential explanations for the occurrence of different cortical activation profiles.

The observation of different profiles of spatial activation brings new insights on the influence of pulse shapes on the electrically evoked responses through a CI. An EX profile means that the reduction of the amplitude of one phase (as the ratio of asymmetry increased) allowed an increase in FR and in SA. This indicates that within the

asymmetric pulse shape, either the attenuation in amplitude of a given phase increased the efficiency of the other phase, or increasing the duration of one phase increased its efficiency. A straightforward explanation to account for the EX profile is a reduction of the interactions between the two pulse phases that leads to increase the efficiency of the short-high amplitude phase. Such a reduction of interactions was already observed when the inter-phase gap is very long and led to a decrease in threshold (Carlyon et al. 2005). It is also worth noting that the conceptual model of "2nd chance spiking" (based on the historical concept of spiking facilitation by electric stimulation; see Boulet, et al 2016, Hey et al. 2017) described by Guérit and colleagues (2020) when using two short monophasic pulses within a short inter-pulse interval gives credibility to the hypothesis where the presentation of a second phase of opposite polarity, but high amplitude, in a short time window might have a counteracting effect through interactions. Interactions might also occur between one pulse and the next, as at high ratios of asymmetry, the inter-pulse period is short. This warrants further study, especially in the context of Continuous Interleaved Sampling (CIS) sound-processing schemes.

The local FO profile, which represents 15-25% of the spatial cortical activation among all conditions (see Table 1), corresponds to reduce spatial activation for specific ranges of asymmetry. The existence of these local FO patterns suggests that the interactions between the different pulse phases are not necessarily linear (or have non-linear consequences at the cortical level), and that these non-linearities might be more prominent in some subjects than in others, in correlation with the spiral ganglion health or the quality of the electrode-neuron interface. This also points toward the idea that each phase does not have equal contribution to the interactions. Note that inside our range of activation, cortical responses remained always significant (i.e., 6 SD above spontaneous firing rate) so the interactions occurring between the pulse phases never

rendered the pulse ineffective. What remains to be investigated are the consequences of the interphase interactions at the very first level in the central auditory system, namely the cochlear nucleus. How the internal circuitry of the cochlear nucleus processed the artificial electrical patterns of activation produced by the different shapes of electrical pulses should be explored in the future.

Focalization profiles (FO) are characterized by a reduction of both firing rate and spatial activation as the ratio of asymmetry increased. The most parsimonious explanation for FO profiles of spatial activation is a reduction in the number of SGN recruited, which can occur either at the level of the peripheral terminals or at the level of the soma. However, it can also come from a phenomenon called "cathodal block" (Frijns et al. 1996) at high levels of stimulation. Macherey et al. (2017) highlighted such effect in CI users through psychoacoustics. Here, it might be encountered as an "anodal block" due to the guinea pig model. If such blocking is responsible for the FO profiles, then anodic-first pulses should be either (a) associated with a majority of FO profiles when the cathodic phase is reduced due to the anodal block predominance, or (b) associated with a majority of EX profiles when the anodic phase is reduced due to the anodal block being lifted and resulted in more action potentials. In fact, the ASF pulse shape induced more EX profiles, and the ALF pulse shape did not promote more EX profiles of spatial activation. Altogether, these results suggest that the hypothesis of an "anodal block" seems inappropriate to explain the spatial activation decreases in the guinea pig primary auditory cortex.

### 3.4. Methodological limitations

The animals used in this study were not deafened as they were part of another study regarding the impact of insertion trauma on cortical responsiveness (Partouche et al.

2022). Thus, it is possible that electrophonic responses (as described by Sato et al. 2016 in the inferior colliculus and earlier in the auditory nerve by Van den Honert and Stypulkowski 1987) occurred due to residual hair cells and might have contributed to cortical electrically evoked responses and confound some of our results. However, a subsequent study (Sato et al. 2017) argues that electroacoustic stimulation through electrophonic responses could be complementary to electroneural stimulation in presence of residual hearing. Considering that residual hearing preservation remains a goal in the field of cochlear implantation, it might be relevant to pursue the study of stimulation parameters such as asymmetric pulse shapes in the presence of residual hair cells.

Due to the length of our surgical preparation and testing protocol, we were unable to test all available electrodes and thus only report results obtained with the most apical. Anatomical differences between the base and more apical regions of the cochlea in terms of volume and the electrode-neurons distance might also impact the overall field of stimulation (Avci et al. 2014). Recently, Räth and colleagues (2024) tied residual hearing preservation after cochlear implantation with cochlea volume and potentially other cochlea dimensions. Thus, taken together with our previous point, it seems promising to further study asymmetric pulse shapes with the local anatomy in mind, especially when they have the potential to improve not only hearing restoration but also some aspects of quality of life such as a reduction in facial nerve stimulation (see Konerding et al. 2023, Gärtner et al. 2022, 2023, Eitutis et al. 2022, and Hyppolito et al. 2023).

One can argue that reducing both the firing rate and the spatial activation at fixed charge (24nC/phase) is potentially an indication that asymmetric pulses are less efficient to

activate the auditory pathway than symmetric pulses. In clinical settings this would lead to significant charge increases for threshold and most confortable loudness. Therefore, the asymmetrical pulse shapes might not be useful in clinical practice because higher charge levels would be needed to reach the loudest intensities. However, for a subset of recordings (N=256), we were able to compare growth functions obtained with symmetric or asymmetric pulse shapes (see supplementary figure 1). These data showed that, for anodic-first pulses, thresholds were similar for the 1/1 and the 1/10 ratios, whereas for cathodic-first pulses thresholds were lower thresholds for the 1/10 ratio. These results echo those from Quass and Kral (2024) although they only reported similar thresholds for both anodic and cathodic leading asymmetric pulses. Also note that in both studies, the dynamic range remained the same.

Last, we should also consider that increasing the pulse duration with a long second phase (in our case, 300µsec with a 1/10 ratio) can raise problems, since it can limit the pulse rate at 303Hz across the array, which increases the risk of potential channel interactions by interleaving pulses on multiple electrodes. However, note that the largest effects described here were for the 1/6 ratio, which limits the pulse rate at 500Hz, but remains in the range of clinical devices (250-1000Hz, Di Lella et al. 2010; see also Arora et al, 2024, which proposes that pulse rate can be reduced from 900 to 500Hz without losing hearing performances).

### 3.5. Future directions and clinical implications.

The present study reports effects on cortical spatial activation obtained one to five hours after cochlear implant insertion. Several studies have already demonstrated the relative

instability of eCAP measurement the first week after implantation (Schvartz-Leizac et al. 2019, Pfingst et al. 2015). Thus, it seems necessary to perform chronic experiments to determine if our results can also be observed a few weeks or months after CI insertion. It also remains to be determined if the frequency range reductions in the order of magnitudes of those observed in our study would provide meaningful improvements to frequency discrimination in human subjects. Last, an important question is whether the effects observed here on spatial cortical activation are also observed with animals presenting partial degeneration of the eighth nerve fibers. All these points warrant for the integration of a behavioral paradigm in our future efforts. In this regard, our animal model is relevant to study the consequence of CI stimulation on higher levels of the auditory system (Middlebrooks 2004) and to propose new paradigms of stimulation to test in CI users. An important point to consider is that stimulation parameters such as asymmetric pulse shapes are part of a multifactorial field in which every aspect of the stimulation, and external factors (such as unwanted side effects, battery life, tinnitus), end up interacting with others. Very few studies quantified parameters interactions (see for example Quass & Kral 2024) and for this reason, coupled with the discussed points above, it is not possible to infer potential benefits, or disadvantages, of asymmetric pulses in CI recipients solely on our results. Although these procedures remain difficult to implement in clinical settings, alternative pulse shapes might still be good candidates to further improve personalization (or tailored fitting) as we demonstrated that they impact the highest level in the auditory pathway (see also Partouche et al 2023 for effects of alternative pulse shapes). In fact, the observation of potentially stronger reduction at intermediate ratios of asymmetry on an animal-to-animal basis also echoes recent findings about personalized fitting. Several studies have already shown that a certain degree of personalization over different aspects of electrical stimulation can be

beneficial (see for example Jahn et al, 2021, Pieper et al. 2020). Two studies (Goehring et al. 2019; Jahn & Arenberg 2019) have proposed an electrode selection method based on the polarity effect to improve speech perception and the spectro-temporal resolution. Our study suggests that modification of the pulse shape might benefit CI users by promoting more focal activation sites at high levels of stimulation but effects on other sound aspects (such as loudness perception and its relationship with stimulation pulse rates (Azadpour et al 2018, Middlebrooks 2008)) still need to be further explored. Most likely, the best strategy for each patient will be a series of trade-offs between the characterized effects of available parameters, their practical implementation, and patient background.

## References


Adenis V, Gourévitch B, Mamelle E, Recugnat M, Stahl P, Gnansia D, Nguyen Y, Edeline JM (2018) ECAP growth function to increasing pulse amplitude or pulse duration demonstrates large inter-animal variability that is reflected in auditory cortex of the guinea pig. PLoS One 13(8):e0201771. https://doi.org/10.1371/journal.pone.0201771

Arenberg JG, Parkinson WS, Litvak L, Chen C, Kreft HA, Oxenham AJ (2018) A Dynamically Focusing Cochlear Implant Strategy Can Improve Vowel Identification in Noise. Ear Hear. 39(6):1136-1145. https://doi.org/10.1097/AUD.0000000000000566

Arnoldner C, Riss D, Kaider A, Mair A, Wagenblast J, Baumgartner WD, Gstöttner W, Hamzavi JS (2008) The intensity-pitch relation revisited: monopolar versus bipolar cochlear stimulation. Laryngoscope. 118(9):1630-6. https://doi.org/10.1097/MLG.0b013e3181799715

Arora K, Plant K, Dawson P, Cowan R (2024) Effect of reducing electrical stimulation rate on hearing performance of Nucleus® cochlear implant recipients. Int J Audiol. Feb 29:1-10. doi: 10.1080/14992027.2024.2314620. Epub ahead of print. PMID: 38420783.

Aushana Y, Souffi S, Edeline JM, Lorenzi C, Huetz C (2018) Robust Neuronal Discrimination in Primary Auditory Cortex Despite Degradations of Spectro-temporal Acoustic Details: Comparison Between Guinea Pigs with Normal Hearing and Mild Age-Related Hearing Loss. J Assoc Res Otolaryngol. 19(2):163-180. https://doi.org/10.1007/s10162-017-0649-1

Avci E, Nauwelaers T, Lenarz T, Hamacher V, Kral A (2014) Variations in microanatomy of the human cochlea. J Comp Neurol. Oct 1;522(14):3245-61. doi: 10.1002/cne.23594. Epub 2014 Apr 12. PMID: 24668424; PMCID: PMC4265794.

Azadpour M, McKay CM, Svirsky MA (2018) Effect of Pulse Rate on Loudness Discrimination in Cochlear Implant Users. J Assoc Res Otolaryngol. Jun;19(3):287-299. doi: 10.1007/s10162-018-0658-8. Epub 2018 Mar 12. PMID: 29532190; PMCID: PMC5962473.

Bahmer A, Baumann U (2016) The Underlying Mechanism of Preventing Facial Nerve Stimulation by Triphasic Pulse Stimulation in Cochlear Implant Users Assessed With Objective Measure. Otol Neurotol. 37(9):1231-7. https://doi.org/10.1097/MAO.0000000000001156

Bahmer A, Adel Y, Baumann U (2017) Preventing Facial Nerve Stimulation by Triphasic Pulse Stimulation in Cochlear Implant Users: Intraoperative Recordings. Otol Neurotol. Dec;38(10):e438-e444. doi: 10.1097/MAO.0000000000001603.

Ballestero J, Recugnat M, Laudanski J, Smith KE, Jagger DJ, Gnansia D, McAlpine D (2015) Reducing Current Spread by Use of a Novel Pulse Shape for Electrical Stimulation of the Auditory Nerve. Trends Hear. 30;19. https://doi.org/10.1177/2331216515619763

Bierer JA, Middlebrooks JC (2002) Auditory cortical images of cochlear-implant stimuli: dependence on electrode configuration. J Neurophysiol. 87(1):478-92. https://doi.org/10.1152/jn.00212.2001

Bierer JA (2010) Probing the electrode-neuron interface with focused cochlear implant stimulation. Trends Amplif. 14(2):84-95. https://doi.org/10.1177/1084713810375249

Bierer JA, Bierer SM, Middlebrooks JC (2010) Partial tripolar cochlear implant stimulation: Spread of excitation and forward masking in the inferior colliculus. Hear Res. 270(1-2):134-42. https://doi.org/10.1016/j.heares.2010.08.006

Bierer JA, Faulkner KF, Tremblay KL (2011) Identifying cochlear implant channels with poor electrode-neuron interfaces: electrically evoked auditory brain stem responses measured with the partial tripolar configuration. Ear Hear. 32(4):436-44. https://doi.org/10.1097/AUD.0b013e3181ff33ab

Bierer JA, Litvak L (2016) Reducing Channel Interaction Through Cochlear Implant Programming May Improve Speech Perception: Current Focusing and Channel Deactivation. Trends Hear. 17; 20. https://doi.org/10.1177/2331216516653389.

Bieszczad KM, Weinberger NM (2010) Representational gain in cortical area underlies increase of memory strength. Proc Natl Acad Sci USA. Feb 23;107(8):3793-8. doi: 10.1073/pnas.1000159107. Epub 2010 Feb 4. Erratum in: Proc Natl Acad Sci U S A. 2013 Mar 26;110(13):5269. PMID: 20133679; PMCID: PMC2840533.

Bingabr MG, Espinoza-Varas B, Sigdel S (2014) Measurements of monopolar and bipolar current spreads using forward-masking with a fixed probe. Cochlear Implants Int. 15(3):166-72. https://doi.org/10.1179/1754762814Y.0000000065

Boulet J, White M, Bruce IC (2016) Temporal Considerations for Stimulating Spiral Ganglion Neurons with Cochlear Implants. J Assoc Res Otolaryngol. Feb;17(1):1-17. doi: 10.1007/s10162-015-0545-5. PMID: 26501873; PMCID: PMC4722016.

Brummer SB, Turner MJ (1977) Electrochemical considerations for safe electrical stimulation of the nervous system with platinum electrodes. IEEE Trans Biomed Eng. Jan;24(1):59-63. doi: 10.1109/TBME.1977.326218. PMID: 851475.

Carlyon RP, van Wieringen A, Deeks JM, Long CJ, Lyzenga J, Wouters J (2005) Effect of inter-phase gap on the sensitivity of cochlear implant users to electrical stimulation. Hear Res. 205(1-2):210-24. https://doi.org/10.1016/j.heares.2005.03.021

Carlyon RP, Deeks JM, McKay CM (2015) Effect of Pulse Rate and Polarity on the Sensitivity of Auditory Brainstem and Cochlear Implant Users to Electrical Stimulation. J Assoc Res Otolaryngol. 16(5):653-68. https://doi.org/10.1007/s10162-015-0530-z

Carlyon RP, Cosentino S, Deeks JM, Parkinson W, Arenberg JG (2018) Effect of Stimulus Polarity on Detection Thresholds in Cochlear Implant Users: Relationships with Average Threshold, Gap Detection, and Rate Discrimination. J Assoc Res Otolaryngol. 19(5):559-567. https://doi.org/10.1007/s10162-018-0677-5

Chari DA, Jiradejvong P, Limb CJ (2019) Tripolar Stimulation Improves Polyphonic Pitch Detection in Cochlear Implant Users. Otol Neurotol. Jan;40(1):38-46. doi: 10.1097/MAO.0000000000002061. PMID: 30531636.

Chatterjee M, Shannon RV (1998) Forward masked excitation patterns in multielectrode electrical stimulation. J Acoust Soc Am. 103(5 Pt 1):2565-72. https://doi.org/10.1121/1.422777

Chua TE, Bachman M, Zeng FG (2011) Intensity coding in electric hearing: effects of electrode configurations and stimulation waveforms. Ear Hear. 32(6):679-89. https://doi.org/10.1097/AUD.0b013e31821a47df

Cohen LT, Busby PA, Whitford LA, Clark GM (1996) Cochlear implant place psychophysics 1. Pitch estimation with deeply inserted electrodes. Audiol Neurootol. 1(5):265-77. https://doi.org/10.1159/000259210

Cohen LT, Saunders E, Clark GM (2001) Psychophysics of a prototype peri-modiolar cochlear implant electrode array. Hear Res. 155(1-2):63-81. https://doi.org/10.1016/s0378-5955(01)00248-9

Cohen LT, Richardson LM, Saunders E, Cowan RS (2003) Spatial spread of neural excitation in cochlear implant recipients: comparison of improved ECAP method and psychophysical forward masking. Hear Res. 179(1-2):72-87. https://doi.org/10.1016/s0378-5955(03)00096-0

DeVries L, Scheperle R, Bierer JA (2016) Assessing the Electrode-Neuron Interface with the Electrically Evoked Compound Action Potential, Electrode Position, and Behavioral Thresholds. J Assoc Res Otolaryngol. 17(3):237-52. https://doi.org/10.1007/s10162-016-0557-9

Di Lella F, Bacciu A, Pasanisi E, Vincenti V, Guida M, Bacciu S (2010) Main peak interleaved sampling (MPIS) strategy: effect of stimulation rate variations on speech perception in adult cochlear implant recipients using the Digisonic SP cochlear implant. Acta Otolaryngol. 130(1):102-7. doi: 10.3109/00016480902896113. PMID: 19424919.

Edeline J-M (1999). Learning-induced physiological plasticity in the thalamo-cortical sensory system: A critical evalutation of receptive field plasticity and maps changes and their potential mechanisms. Progress in Neurobiolology, 57, 165-224

Edeline J-M (2003). The thalamo-cortical auditory receptive fields: Regulation by the states of vigilance, learning and the neuromodulatory systems. Experimental Brain Research, 153, 554-572.

Edeline JM, Dutrieux G, Manunta Y, Hennevin E (2001) Diversity of receptive field changes in auditory cortex during natural sleep. Eur J Neurosci. 14(11):1865-80. https://doi.org/10.1046/j.0953-816x.2001.01821.x

Eisen MD, Franck KH (2005) Electrode interaction in pediatric cochlear implant subjects. J Assoc Res Otolaryngol. 6(2):160-70. https://doi.org/10.1007/s10162-005-5057-2

Eitutis ST, Carlyon RP, Tam YC, Salorio-Corbetto M, Vanat Z, Tebbutt K, Bardsley R, Powell HRF, Chowdhury S, Tysome JR, Bance ML (2022) Management of Severe Facial Nerve Cross Stimulation by Cochlear Implant Replacement to Change Pulse Shape and Grounding Configuration: A Case-series. Otol Neurotol. 2022 Apr 1;43(4):452-459. doi: 10.1097/MAO.0000000000003493.

Frijns JH, de Snoo SL, ten Kate JH (1996) Spatial selectivity in a rotationally symmetric model of the electrically stimulated cochlea. Hear Res. 95(1-2):33-48. https://doi.org/10.1016/0378-5955(96)00004-4

Frijns JH, Briaire JJ, de Laat JA, Grote JJ (2002) Initial evaluation of the Clarion CII cochlear implant: speech perception and neural response imaging. Ear Hear. 23(3):184-97. https://doi.org/10.1097/00003446-200206000-00003

Gärtner L, Backus BC, Le Goff N, Morgenstern A, Lenarz T, Büchner A (2023) Cochlear Implant Stimulation Parameters Play a Key Role in Reducing Facial Nerve Stimulation. J Clin Med. Sep 25;12(19):6194. doi: 10.3390/jcm12196194.

Gärtner L, Lenarz T, Ivanauskaite J, Büchner A (2022). Facial nerve stimulation in cochlear implant users - a matter of stimulus parameters? Cochlear Implants Int. May;23(3):165-172. doi: 10.1080/14670100.2022.2026025.

Gaucher Q, Edeline JM, Gourévitch B (2012) How different are the local field potentials and spiking activities? Insights from multi-electrodes arrays. J Physiol Paris. 106(3-4):93-103. https://doi.org/10.1016/j.jphysparis.2011.09.006

Gaucher Q, Huetz C, Gourévitch B, Edeline JM (2013) Cortical inhibition reduces information redundancy at presentation of communication sounds in the primary auditory cortex. J Neurosci. 26;33(26):10713-28. https://doi.org/10.1523/JNEUROSCI.0079-13.2013

Gladwin TE (2020). An implementation of repeated measures ANOVA: effect coding, automated exploration of interactions, and randomization testing. MethodsX, doi:10.1016/j.mex.2020.100947.

Goehring T, Archer-Boyd A, Deeks JM, Arenberg JG, Carlyon RP (2019) A Site-Selection Strategy Based on Polarity Sensitivity for Cochlear Implants: Effects on Spectro-Temporal Resolution and Speech Perception. J Assoc Res Otolaryngol. 20(4):431-448. https://doi.org/10.1007/s10162-019-00724-4

Goldwyn JH, Bierer SM, Bierer JA (2010) Modeling the electrode-neuron interface of cochlear implants: effects of neural survival, electrode placement, and the partial tripolar configuration. Hear Res. 1;268(1-2):93-104. https://doi.org/10.1016/j.heares.2010.05.005

Gourévitch B, Doisy T, Avillac M, Edeline JM (2009) Follow-up of latency and threshold shifts of auditory brainstem responses after single and interrupted acoustic trauma in guinea pig. Brain Res. 1304:66-79. https://doi.org/10.1016/j.brainres.2009.09.041

Gourévitch B, Edeline JM (2011) Age-related changes in the guinea pig auditory cortex: relationship with brainstem changes and comparison with tone-induced hearing loss. Eur J Neurosci. 34(12):1953-65. https://doi.org/10.1111/j.1460-9568.2011.07905.x

Guérit F, Marozeau J, Deeks JM, Epp B, Carlyon RP (2018) Effects of the relative timing of opposite-polarity pulses on loudness for cochlear implant listeners. J Acoust Soc Am. 144(5):2751. https://doi.org/10.1121/1.5070150

Guérit F, Marozeau J, Epp B, Carlyon RP (2020) Effect of the Relative Timing between Same-Polarity Pulses on Thresholds and Loudness in Cochlear Implant Users. J Assoc Res Otolaryngol. Dec;21(6):497-510. doi: 10.1007/s10162-020-00767-y. Epub 2020 Aug 24. PMID: 32833160; PMCID: PMC7644659.

Heshmat A, Sajedi S, Schrott-Fischer A, Rattay F (2021) Polarity Sensitivity of Human Auditory Nerve Fibers Based on Pulse Shape, Cochlear Implant Stimulation Strategy and Array. Front Neurosci. Dec 8;15:751599. doi: 10.3389/fnins.2021.751599. PMID: 34955717; PMCID: PMC8692583.

Hey M, Müller-Deile J, Hessel H, Killian M (2017) Facilitation and refractoriness of the electrically evoked compound action potential. Hear Res. Nov;355:14-22. doi: 10.1016/j.heares.2017.09.001. Epub 2017 Sep 11. PMID: 28947082.

Hughes ML, Stille LJ (2008) Psychophysical versus physiological spatial forward masking and the relation to speech perception in cochlear implants. Ear Hear. 29(3):435-52. https://doi.org/10.1097/AUD.0b013e31816a0d3d

Hughes ML, Stille LJ (2010) Effect of stimulus and recording parameters on spatial spread of excitation and masking patterns obtained with the electrically evoked compound action potential in cochlear implants. Ear Hear. 31(5): 679-92. https://doi.org/10.1097/AUD.0b013e3181e1d19e

Hughes ML, Goehring JL, Baudhuin JL (2017) Effects of Stimulus Polarity and Artifact Reduction Method on the Electrically Evoked Compound Action Potential. Ear Hear. 38(3):332-343. https://doi.org/10.1097/AUD.0000000000000392

Hughes ML, Choi S, Glickman E (2018) What can stimulus polarity and interphase gap tell us about auditory nerve function in cochlear-implant recipients? Hear Res. 359:50-63. https://doi.org/10.1016/j.heares.2017.12.015

Hyppolito MA, Barbosa Reis ACM, Danieli F, Hussain R, Le Goff N (2023) Cochlear re-implantation with the use of multi-mode grounding associated with anodic monophasic pulses to manage abnormal facial nerve stimulation. Cochlear Implants Int. Mar;24(2):55-64. doi: 10.1080/14670100.2022.2157077.

Jahn KN, Arenberg JG (2019) Evaluating Psychophysical Polarity Sensitivity as an Indirect Estimate of Neural Status in Cochlear Implant Listeners. J Assoc Res Otolaryngol. 20(4):415-430. https://doi.org/10.1007/s10162-019-00718-2

Jahn KN, Arenberg JG (2020) Identifying Cochlear Implant Channels With Relatively Poor Electrode-Neuron Interfaces Using the Electrically Evoked Compound Action Potential. Ear Hear. Jul/Aug;41(4):961-973. doi: 10.1097/AUD.0000000000000844. PMID: 31972772; PMCID: PMC10443089.

Javel E, Shepherd RK (2000) Electrical stimulation of the auditory nerve. III. Response initiation sites and temporal fine structure. Hear Res. 140(1-2):45-76. https://doi.org/10.1016/s0378-5955(99)00186-0

Konerding WS, Baumhoff P, Kral A (2023) Anodic Polarity Minimizes Facial Nerve Stimulation as a Side Effect of Cochlear Implantation. J Assoc Res Otolaryngol. Feb;24(1):31-46. doi: 10.1007/s10162-022-00878-8. Epub 2022 Dec 2. PMID: 36459250; PMCID: PMC9971531.

Lilly JC, Hughes JR, Alvord EC, Galkin, TW (1955) Brief, Noninjurious Electric Waveform for Stimulation of the Brain. Science 121(3144), 468–469. http://www.jstor.org/stable/1681665

Lim HH, Tong YC, Clark GM (1989) Forward masking patterns produced by intracochlear electrical stimulation of one and two electrode pairs in the human cochlea. J Acoust Soc Am. 86(3):971-80. https://doi.org/10.1121/1.398732

Loeb GE, White MW, Jenkins WM (1983) Biophysical considerations in electrical stimulation of the auditory nervous system. Ann N Y Acad Sci. 405:123-36. doi: 10.1111/j.1749-6632.1983.tb31625.x. PMID: 6575638.

Macherey O, van Wieringen A, Carlyon RP, Deeks JM, Wouters J (2006) Asymmetric pulses in cochlear implants: effects of pulse shape, polarity, and rate. J Assoc Res Otolaryngol. 7(3):253-66. https://doi.org/10.1007/s10162-006-0040-0

Macherey O, Carlyon RP, van Wieringen A, Deeks JM, Wouters J (2008) Higher sensitivity of human auditory nerve fibers to positive electrical currents. J Assoc Res Otolaryngol. 9(2):241-51. https://doi.org/10.1007/s10162-008-0112-4

Macherey O, Carlyon RP, Chatron J, Roman S (2017) Effect of Pulse Polarity on Thresholds and on Non-monotonic Loudness Growth in Cochlear Implant Users. J Assoc Res Otolaryngol. 18(3):513-527. https://doi.org/10.1007/s10162-016-0614-4

Manunta Y, Edeline JM (1999) Effects of noradrenaline on frequency tuning of auditory cortex neurons during wakefulness and slow-wave sleep. Eur J Neurosci. 11(6):2134-50. https://doi.org/10.1046/j.1460-9568.1999.00633.x

McHardy J, Robblee LS, Marston JM, Brummer SB (1980) Electrical stimulation with pt electrodes. IV. Factors influencing Pt dissolution in inorganic saline. Biomaterials. Jul;1(3):129-34. doi: 10.1016/0142-9612(80)90034-4. PMID: 7470563.

McKay CM, O'Brien A, James CJ (1999) Effect of current level on electrode discrimination in electrical stimulation. Hear Res. 136(1-2):159-64. https://doi.org/10.1016/s0378-5955(99)00121-5

McKay CM, Chandan K, Akhoun I, Siciliano C, Kluk K (2013) Can ECAP measures be used for totally objective programming of cochlear implants? J Assoc Res Otolaryngol. 14(6):879-90. https://doi.org/10.1007/s10162-013-0417-9

Mesnildrey Q, Venail F, Carlyon RP, Macherey O (2020) Polarity Sensitivity as a Potential Correlate of Neural Degeneration in Cochlear Implant Users. J Assoc Res Otolaryngol. https://doi.org/10.1007/s10162-020-00742-7

Middlebrooks JC (2004) Effects of cochlear-implant pulse rate and inter-channel timing on channel interactions and thresholds. J Acoust Soc Am. 116(1):452-68. https://doi.org/10.1121/1.1760795

Middlebrooks JC (2008) Cochlear-implant high pulse rate and narrow electrode configuration impair transmission of temporal information to the auditory cortex. J Neurophysiol. 100(1):92-107. https://doi.org/10.1152/jn.01114.2007

Miller CA, Abbas PJ, Rubinstein JT, Robinson BK, Matsuoka AJ, Woodworth G (1998) Electrically evoked compound action potentials of guinea pig and cat: responses to monopolar, monophasic stimulation. Hear Res. 119(1-2):142-54. https://doi.org/10.1016/s0378-5955(98)00046-x

Miller CA, Abbas PJ, Robinson BK, Rubinstein JT, Matsuoka AJ (1999) Electrically evoked single-fiber action potentials from cat: responses to monopolar, monophasic stimulation. Hear Res. 130(1-2):197-218. https://doi.org/10.1016/s0378-5955(99)00012-x

Miller CA, Robinson BK, Rubinstein JT, Abbas PJ, Runge-Samuelson CL (2001) Auditory nerve responses to monophasic and biphasic electric stimuli. Hear Res. 151(1-2):79-94. https://doi.org/10.1016/s0300-2977(00)00082-6

Miller CA, Abbas PJ, Hay-McCutcheon MJ, Robinson BK, Nourski KV, Jeng FC (2004) Intracochlear and extracochlear ECAPs suggest antidromic action potentials. Hear Res. 198(1-2):75-86. https://doi.org/10.1016/j.heares.2004.07.005

Navntoft CA, Marozeau J, Barkat TR (2020) Ramped pulse shapes are more efficient for cochlear implant stimulation in an animal model. Sci Rep. 24;10(1):3288. https://doi.org/10.1038/s41598-020-60181-5

Nguyen Y, Miroir M, Kazmitcheff G, Sutter J, Bensidhoum M, Ferrary E, Sterkers O, Bozorg Grayeli A. (2012) Cochlear implant insertion forces in microdissected human cochlea to evaluate a prototype array. Audiol Neurootol.;17(5):290-8.

Occelli F, Suied C, Pressnitzer D, Edeline JM, Gourévitch B (2016) A Neural Substrate for Rapid Timbre Recognition? Neural and Behavioral Discrimination of Very Brief Acoustic Vowels. Cereb Cortex. 26(6):2483-2496. https://doi.org/10.1093/cercor/bhv071

Partouche E, Adenis V, Gnansia D, Stahl P, Edeline JM (2022) Increased Threshold and Reduced Firing Rate of Auditory Cortex Neurons after Cochlear Implant Insertion. Brain Sci. Jan 31;12(2):205. doi: 10.3390/brainsci12020205. PMID: 35203968; PMCID: PMC8870646.

Partouche E, Adenis V, Stahl P, Huetz C, Edeline JM (2023) What Is the Benefit of Ramped Pulse Shapes for Activating Auditory Cortex Neurons? An Electrophysiological Study in an Animal Model of Cochlear Implant. Brain Sci. Jan 31;13(2):250. doi: 10.3390/brainsci13020250. PMID: 36831793; PMCID: PMC9954719.

Pfingst BE, Hughes AP, Colesa DJ, Watts MM, Strahl SB, Raphael Y (2015) Insertion trauma and recovery of function after cochlear implantation: Evidence from objective functional measures. Hear Res. 330(Pt A):98-105. https://doi.org/10.1016/j.heares.2015.07.010

Pieper SH, Brill S, Bahmer A (2020) Loudness Perception and Dynamic Range Depending on Interphase Gaps of Biphasic Pulses in Cochlear Implants. Ear Hear. Sep/Oct;41(5):1251-1257. doi: 10.1097/AUD.0000000000000843. PMID: 31972773.

Quass GL, Baumhoff P, Gnansia D, Stahl P, Kral A (2020) Level coding by phase duration and asymmetric pulse shape reduce channel interactions in cochlear implants. Hear Res. Oct;396:108070. doi: 10.1016/j.heares.2020.108070. Epub 2020 Sep 4. PMID: 32950954.

Quass GL, Kral A (2024) Tripolar configuration and pulse shape in cochlear implants reduce channel interactions in the temporal domain. Hear Res. Mar 1;443:108953. doi: 10.1016/j.heares.2024.108953. Epub 2024 Jan 19. PMID: 38277881.

Räth M, Schurzig D, Timm ME, Lenarz T, Warnecke A (2024) Correlation of Scalar Cochlear Volume and Hearing Preservation in Cochlear Implant Recipients with Residual Hearing. Otol Neurotol. Mar 1;45(3):256-265. doi: 10.1097/MAO.0000000000004122. Epub 2024 Jan 24. PMID: 38361293.

Rattay F, Lutter P, Felix H (2001) A model of the electrically excited human cochlear neuron. I. Contribution of neural substructures to the generation and propagation of spikes. Hear Res. 153(1-2):43-63. https://doi.org/10.1016/s0378-5955(00)00256-2

Rattay F, Leao RN, Felix H (2001) A model of the electrically excited human cochlear neuron. II. Influence of the three-dimensional cochlear structure on neural excitability. Hear Res. 153(1-2):64-79. https://doi.org/10.1016/s0378-5955(00)00257-4

Recanzone GH, Schreiner CE, Merzenich MM. (1993) Plasticity in the frequency representation of primary auditory cortex following discrimination training in adult owl monkeys. J Neurosci. 13(1):87-103.

Reed A, Riley J, Carraway R, Carrasco A, Perez C, Jakkamsetti V, Kilgard MP (2011) Cortical map plasticity improves learning but is not necessary for improved performance. Neuron. Apr 14;70(1):121-31. doi: 10.1016/j.neuron.2011.02.038. PMID: 21482361.

Resnick JM, O'Brien GE, Rubinstein JT (2018) Simulated auditory nerve axon demyelination alters sensitivity and response timing to extracellular stimulation. Hear Res. 361:121-137. https://doi.org/10.1016/j.heares.2018.01.014

Rutkowski RG, Weinberger NM. (2005) Encoding of learned importance of sound by magnitude of representational area in primary auditory cortex. Proc Natl Acad Sci U S A.;102(38):13664-9.

Sato M, Baumhoff P, Kral A (2016) Cochlear Implant Stimulation of a Hearing Ear Generates Separate Electrophonic and Electroneural Responses. J Neurosci. Jan 6;36(1):54-64. doi: 10.1523/JNEUROSCI.2968-15.2016. PMID: 26740649; PMCID: PMC4717149.

Sato M, Baumhoff P, Tillein J, Kral A (2017) Physiological Mechanisms in Combined Electric-Acoustic Stimulation. Otol Neurotol. Sep;38(8):e215-e223. doi: 10.1097/MAO.0000000000001428. PMID: 28806329.

Schvartz-Leyzac KC, Zwolan TA, Pfingst BE (2017) Effects of electrode deactivation on speech recognition in multichannel cochlear implant recipients. Cochlear Implants Int. 18(6):324-334. https://doi.org/10.1080/14670100.2017.1359457

Schvartz-Leyzac KC, Colesa DJ, Buswinka CJ, Swiderski DL, Raphael Y, Pfingst BE (2019) Changes over time in the electrically evoked compound action potential (ECAP) interphase gap (IPG) effect following cochlear implantation in Guinea pigs. Hear Res. 383:107809. https://doi.org/10.1016/j.heares.2019.107809

Seyyedi M, Eddington DK, Nadol JB Jr (2013) Effect of monopolar and bipolar electric stimulation on survival and size of human spiral ganglion cells as studied by postmortem histopathology. Hear Res. 302:9-16. https://doi.org/10.1016/j.heares.2013.04.007

Shannon RV (1983) Multichannel electrical stimulation of the auditory nerve in man. II. Channel interaction. Hear Res. 12(1):1-16. https://doi.org/10.1016/0378-5955(83)90115-6

Souffi S, Lorenzi C, Huetz C Edeline JM (2020) Noise-sensitive but more precise subcortical representations co-exist with robust cortical encoding of natural vocalizations. J. Neuroscience. 40, 5228-5246. https://doi.org/10.1523/jneurosci.2731-19.2020

Souffi S, Lorenzi C, Huetz C & Edeline JM (2021) Robustness to noise in the auditory system: A distributed and predictable property. eNeuro. Mar 18; 8(2):ENEURO.0043-21.2021. https://doi.org/10.1523/eneuro.0043-21.2021

Spitzer ER, Hughes ML (2017) Effect of Stimulus Polarity on Physiological Spread of Excitation in Cochlear Implants. J Am Acad Audiol. 28(9):786-798. https://doi.org/10.3766/jaaa.16144

Spitzer ER, Choi S, Hughes ML (2019) The Effect of Stimulus Polarity on the Relation Between Pitch Ranking and ECAP Spread of Excitation in Cochlear Implant Users. J Assoc Res Otolaryngol. 20(3):279-290. https://doi.org/10.1007/s10162-018-00712-0

Srinivasan AG, Padilla M, Shannon RV, Landsberger DM (2014) Improving speech perception in noise with current focusing in cochlear implant users. Hear Res. 299:29-36. https://doi.org/10.1016/j.heares.2013.02.004

Todd AE, Landsberger DM (2018) The effect of polarity order and electrode-activation order on loudness in cochlear implant users. J Acoust Soc Am. 144(2):EL112. https://doi.org/10.1121/1.5049701

Tong YC, Clark GM (1986) Loudness summation, masking, and temporal interaction for sensations produced by electric stimulation of two sites in the human cochlea. J Acoust Soc Am. 79(6):1958-66. https://doi.org/10.1121/1.393203

Undurraga JA, van Wieringen A, Carlyon RP, Macherey O, Wouters J (2010) Polarity effects on neural responses of the electrically stimulated auditory nerve at different cochlear sites. Hear Res. 1;269(1-2):146-61. https://doi.org/10.1016/j.heares.2010.06.017

Undurraga JA, Carlyon RP, Wouters J, van Wieringen A (2013) The polarity sensitivity of the electrically stimulated human auditory nerve measured at the level of the brainstem. J Assoc Res Otolaryngol. 14(3):359-77. https://doi.org/10.1007/s10162-013-0377-0

van den Honert C, Stypulkowski PH (1987) Single fiber mapping of spatial excitation patterns in the electrically stimulated auditory nerve. Hear Res.29:195–206. https://doi.org/10.1016/0378-5955(87)90167-5

van Wieringen A, Carlyon RP, Laneau J, Wouters J (2005) Effects of waveform shape on human sensitivity to electrical stimulation of the inner ear. Hear Res. 200(1-2):73-86. https://doi.org/10.1016/j.heares.2004.08.006

van Wieringen A, Macherey O, Carlyon RP, Deeks JM, Wouters J (2008) Alternative pulse shapes in electrical hearing. Hear Res. 242(1-2):154-63. https://doi.org/10.1016/j.heares.2008.03.005

Wallace MN, Palmer AR. (2008) Laminar differences in the response properties of cells in the primary auditory cortex. Exp Brain Res.; 184(2):179-91. doi: 10.1007/s00221-007-1092-z.

Wallace MN, Rutkowski RG, Palmer AR (2000) Identification and localisation of auditory areas in guinea pig cortex. Exp Brain Res. 132(4):445-56. https://doi.org/10.1007/s002210000362

Wobbrock JO, Findlater L, Gergle D, Higgins JJ (2011). The aligned rank transform for nonparametric factorial analyses using only ANOVA procedures. Proceedings of the ACM Conference on Human Factors in Computing Systems (CHI '11). Vancouver, British Columbia (May 7-12, 2011). New York: ACM Press, pp. 143-146.

Zhou N, Pfingst BE (2014) Effects of site-specific level adjustments on speech recognition with cochlear implants. Ear Hear. 35(1):30-40. https://doi.org/10.1097/AUD.0b013e31829d15cc

Zhu Z, Tang Q, Zeng FG, Guan T, Ye D (2012) Cochlear-implant spatial selectivity with monopolar, bipolar and tripolar stimulation. Hear Res. 283(1-2):45-58. https://doi.org/10.1016/j.heares.2011.11.005

## Figure Legends

**Figure 1.** Schematic diagrams representing the different pulses configurations used in our study.

A. Schematic comparison between the shape of the square symmetric pulse with a 1/1 ratio and the most asymmetric pulse shape (1/10) where the amplitude of the second phase was 1/10 of the first (and its duration 10 times longer for keeping the charge balanced).
B. Representation of the four pulse configurations used in the present study depending on whether the first phase was short (ASF and CSF) or long (ALF and CLF) for both tested polarities. ASF: Anodic Short First. CSF: Cathodic Short First. ALF: Anodic Long First. CLF: Cathodic Long First.

**Figure 2.** Example of tonotopic organization in the primary auditory cortex based on spectrotemporal receptive fields.

Simultaneous recordings were obtained in the guinea pig primary auditory cortex at eight different locations. The MultiUnit Activity (MUA) was recorded with an array of 8 electrodes placed along the rostro-caudal axis. Spectrotemporal receptive fields were obtained by presenting pure tones from 140Hz to 36kHz. White contour circles indicate evoked firing rates above spontaneous activity plus 6 SD. Note that the receptive fields are from low to high frequencies when progressing from the rostral to the caudal part of A1.

**Figure 3.** Comparison between the effects generated by the Monopolar (MP) and the Bipolar (BP) stimulation mode at the level of A1.

A. Scattergrams comparing the evoked firing rates (FR in spike/sec) obtained at 31.5nC using monopolar (MP, abscissa) vs. bipolar (BP, ordinates) stimulation mode for anodic-first (Top left) and cathodic-first pulse (Bottom left). On average, BP evoked lower FR than MP for both polarity schemes.

B. Scattergrams comparing the spatial activations (in mm) obtained at 31.5nC using either MP (abscissa) or BP (ordinates) stimulation mode for anodic-first (Top right) and cathodic-first pulse (Bottom right). On average, BP evoked smaller SA than MP with both polarity schemes.

**Figure 4**. Raster plots (A) and quantification of evoked responses (B) for two individual recordings.

A. Raster plots of two individual recording sites showing evoked responses triggered by each ratio of asymmetry (from 1/1, bottom to 1/10, top) for the ASF shape (A1, A2). Alternating colors represent the different levels of asymmetry with the 64 repetitions of for each level.
B. Corresponding mean evoked firing rates (spikes/sec) observed for these two recordings (black curves) and their associated standard deviation (purple field) for each ratio tested (top and bottom curves correspond respectively to left and right raster plots). Red

circles indicate the maximum observed FR. In both case, the mean FR decreased as the ratio of asymmetry increased, with ratio 1/1 (symmetric pulse) evoking the maximum firing rate.

**Figure 5.** Evolution of cortical evoked firing rate as a function of the pulse asymmetry.

For each asymmetric pulse shape tested (ASF: black, CSF: brown, ALF: grey, CLF: yellow), evolutions of the mean evoked firing rate (+SEM) are represented as percentages using the symmetric pulse shape (ratio 1/1) as a reference point. In general, all asymmetric pulse shapes evoked lower firing rates as the ratio of asymmetry increased. The magnitude of the reduction however differed within each pulse shape (maxima: 23% decrease for ASF, 24% decrease for ALF, 26% decrease for CLF at ratio 1/6 and 27% decrease for CSF at ratio 1/7).

**Figure 6.** Individual examples of firing rate decrease (A.) and spatial focalization of cortical activation (B.) for the different ratios of asymmetry.

A. The mean evoked firing rate (FR) of two cortical sites is plotted as a function of the asymmetry ratio from the 1/1 symmetrical ratio to the 1/10. For these two examples, the FR decreased whatever the pulse configuration was (left: ASF, right: CSF).
B. Cortical spatial activation obtained for the different ratios of asymmetry from the 1/1 to the 1/10. The two examples displayed in A correspond to the cortical activation displayed in B (Left: ASF, right: CSF). There was a clear reduction in cortical spatial activation when the asymmetry ratio increased (from 0.95 to 0.75 mm with the ASF and from 1.5 to 0.9 with the CSF).

**Figure 7.** Group data showing decreased firing rate (A) and frequency range (B) with the use of asymmetric pulse shapes. In both cases, except for ASF, most recordings showed lower values for asymmetric pulse shapes.

A. Scattergrams comparing the mean firing rates observed between ratios 1/1 and 1/10, for each asymmetric pulse shape tested (from left to right: ASF, CSF, ALF, CLF). The red line is the equality line.
B. Scattergrams comparing the frequency ranges (in octaves) covered by spatial activation between ratios 1/1 and 1/10 for each asymmetric pulse shape tested (same order as A). Red line represents the equality line. Note that reductions of frequency range up to 0.6 octaves have been observed.

**Figure 8.** Individual examples illustrating the three profiles of spatial activation (A-C) obtained when changing the ratio of asymmetry.

A. The focalization category (FO) represented a reduction of the firing rate and spatial activation at the 1/10 ratio compared with the 1/1 ratio. CSF shape used.

B. The expansion category (EX) represented an increase of the firing rate and an enlargement of the spatial activation at the 1/10 ratio compared with the 1/1 ratio. ASF shape used.
C. The local focalization category (called L-FO) represented a maximal reduction of the firing rate and spatial activation at a particular ratio of asymmetry (instead of the ratio 1/10) compared with the 1/1 ratio. ALF shape used.

**Supplementary Figure 1.** Cortical growth functions presented as percentages of changes in evoked firing rate for an injected charge ranging from 3 to 31.5nC with symmetric (1/1) or asymmetric (1/10) pulse shapes. These growth functions were built from 256 cortical recordings obtained from eight control guinea pigs.

A. Comparison of the growth functions obtained with symmetric (ratio 1/1, black curve) and asymmetric pulse shapes (ratio 1/10, grey curve) for anodic-first pulse, which is equivalent to the ASF pulse shape used in this study. The injected charge evoking the maximum FR for the 1/1 ratio was used for reference (100%). With both ratios, the growth functions are equivalent in terms of threshold and slope meaning that dynamic ranges are the same.

B. Comparison of the growth functions obtained with symmetric (ratio 1/1, black curve) and asymmetric pulse shapes (ratio 1/10, white curve) for cathodic-first pulse, which is equivalent to the CSF pulse shape used in this study. The injected charge evoking the maximum FR for the 1/1 ratio was used for reference (100%). The growth functions are equivalent in terms of threshold and saturation level but the curve with the 1/10 ratio was shifted to the left by 3nC. The asymmetric pulse evoked a higher firing rate than the symmetric pulse, but the thresholds and the slopes of the growth function were not statistically different meaning that dynamics ranges are equivalent.

CRedit authorship contribution Statement.

**Victor Adenis, Pierre Stahl, Dan Gnansia & Jean-Marc Edeline**: Conceptualization, Funding acquisition, Data curation

**Victor Adenis and Elie Partouche**: Investigation; methodology

**Chloé Huetz Elie Partouche and Victor Adenis:** Software analysis, visualization, formal analysis

**Jean-Marc Edeline, Victor Adenis:** Writing : original draft, review and editing

All authors have read and agreed to the published version of the manuscript.

GA